

We are IntechOpen, the world's leading publisher of Open Access books Built by scientists, for scientists

6,900

Open access books available

185,000

International authors and editors

200M

Downloads

Our authors are among the

154

Countries delivered to

TOP 1%

most cited scientists

12.2%

Contributors from top 500 universities



WEB OF SCIENCE™

Selection of our books indexed in the Book Citation Index
in Web of Science™ Core Collection (BKCI)

Interested in publishing with us?
Contact book.department@intechopen.com

Numbers displayed above are based on latest data collected.
For more information visit www.intechopen.com



Validation and Quality Assessment of Sea Levels from SARAL/AltiKa Satellite Altimetry over the Marginal Seas at the Southeast Asia

Noor Nabilah Abdullah and Nurul Hazrina Idris

Additional information is available at the end of the chapter

<http://dx.doi.org/10.5772/intechopen.74399>

Abstract

In this study, high resolution (40 Hz) sea levels derived from the advanced SARAL/AltiKa satellite altimetry are validated over the Southeast Asia coastal regions. The parameter of sea level is derived based on three standard retracking algorithms of MLE-4, Ice-1, and Ice-2. The assessments of quantity and quality of the retracked sea levels are conducted to identify the optimum retracker over the study regions, which are the Andaman Sea, the Strait of Malacca, the South China Sea, the Gulf of Thailand, and the Sulu Sea. The quantitative analysis involves the computation of percentage of data availability and the minimum distance of sea level anomaly (SLA) to the coastline. The qualitative analysis involves the absolute validation with tide gauge. In general, AltiKa measurement can get as close as ~1 km to the coastline with $\geq 85\%$ data availability. The Ice-1 retracker has shown an excellent performance with percentage of data availability $\geq 90\%$ and minimum distance as close as 0.9 km to the coastline. In term of quality of the data, 3 out of 6 validation site show that Ice-1 retracker is superior than the other retracker with temporal correlation up to 0.89 and RMS error up to 8 cm.

Keywords: SARAL/AltiKa, coastal sea level, validation, retracking, Southeast Asia

1. Introduction

Satellite altimeter occupies the radar technology at vertical incidence. It measures the two-way travel time of pulses, which corresponds to the distance between the satellite and the ocean surface. The time between the transmission of the pulses to the reception of the reflected echoes is proportional to the satellite's orbital height. Through the magnitude and shape of

the echoes (or waveform), geophysical information about the ocean surfaces (i.e., sea level, wave height, and wind speed) can be retrieved (**Figure 1**).

There are two types of radar altimetry: pulse-limited and beam-limited. The pulse-limited altimeter dictates the shape of returning signals by the length (width) of the pulse; meanwhile, the beam-limited dictates the shape of returning signals by the width of the beam (cf. [1]). The technology of pulse-limited altimeter has been used over the past 30 years, on-board of various altimetry missions such as ERS series, Jason series, and SARAL/AltiKa. Contrary, the beam-limited altimeter is considered as an advanced technology, which carries delay-Doppler altimeter instrument on-board of Cryosat-2 and Sentinel 3A satellites. With the advanced technology, the improvement can be seen in terms of the along-track spatial resolution, the noise ratio, and the sensitivity rate to the sea states [1].

The altimetry data have been beneficial for measuring ocean geophysical parameters, particularly the sea levels. They have been embedded in several ocean modeling systems such as the Australian national coastal modeling hindcast/forecast systems (e.g., BLUElink), and Regional Ocean Modeling System in Alaska, the United States of America. The altimetry can provide highly accurate sea level measurement (in cm level) over the open ocean due to proper modeling of ocean state qualities (e.g., tides) and accurate measurement of atmospheric refractions [2]. The altimetry is capable of providing accurate information of ocean properties up to 4 cm in height measurements [3, 4] and 2–3 cm in mean sea level variations [5].

However, in coastal regions, altimetry and its applications face many challenges (e.g., [2, 6–9]) due to various reasons. The accuracy of measurements decreases abruptly as the altimeter approaches the coast, where the sea conditions can diverge drastically over time and space. In addition, the altimetric waveforms within a footprint are usually corrupted by land, resulting in complicated ocean signals.

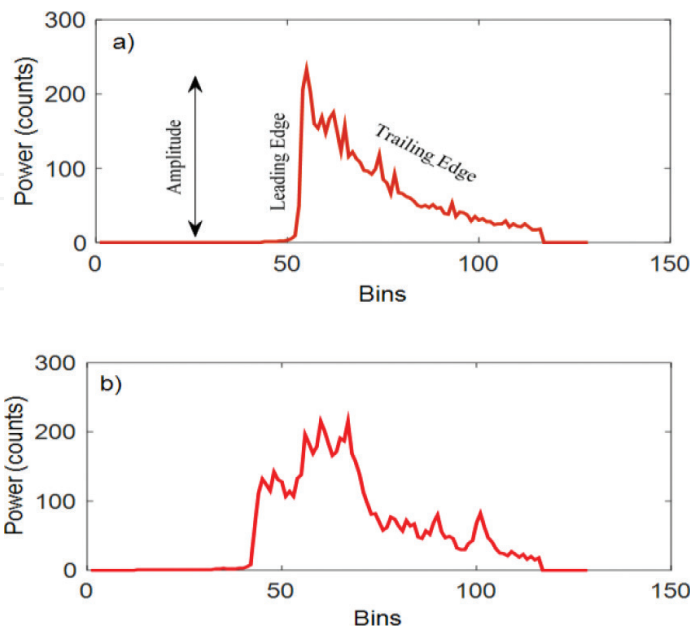


Figure 1. Examples of returned waveforms. (a) Brown-shaped waveform over homogeneous ocean surface. (b) Non-brown waveform over complex coastal area.

Figure 1 shows the altimetric waveforms over the open and coastal oceans. The waveform shape over the open ocean (**Figure 1a**) follows the Brown [10] model. It features a sharp increase of leading edge, following a decreasing plateau. From the shape, several ocean parameters can be deduced. The parameter of wind speed can be deduced from the waveform amplitude, the sea level from the mid-point of leading edge, and the significant wave height from the slope of leading edge. Satellite instrumentation parameters can also be deduced: thermal noise and antenna mispointing angle (based on the slope of trailing edge). In **Figure 1b**, the land impact is clearly seen in the waveform, which features high amplitude on the waveform trailing edge. In case of corrupted waveforms, the processor tracker on-board of the satellite cannot properly determine the ocean parameters. Therefore, an efficient signal post-processing called as “the retracking” should be performed on the ground to optimize the accuracy of the estimation [8]. This is because the leading edge of waveform deviates from the on-board tracking gate [8], thus reducing the accuracy of measurements.

Waveform retracking can be conducted based on the physical (e.g., MLE4, OCE3, and Red3) or empirical (e.g., Ice1 and Offset Centre of Gravity (OCOG)) retrackers. The former fits the waveforms to an ocean surface model (e.g., [10]) to retrieve the optimized parameters (e.g., [10–13, 14]), and the latter retrieves the parameters based on the empirical assumption about the signals (e.g., [15, 16]).

Due to the low quality of altimeter geophysical retrieval over coastal oceans, data are usually systematically flagged and rejected. The coastal water is poorly observed, particularly within ~10 km of the shoreline [17, 18]. The no data gaps over coastal regions have been improved with the advanced altimetric technology such as AltiKa and Sentinel 3A altimetry mission. The AltiKa satellite operates with a Ka-band (~35.8 GHz) frequency signal. It produces a finer spatial resolution when compared to Ku-band (~13.5 GHz). With the smaller size footprint (~8 km in diameter compared to 20 km for Jason-2 and 15 km for Envisat) [19] and higher spatial resolution along the satellite track (40 Hz, compared to 20 Hz for Jason-2), the AltiKa can bring measurements closer to the coastline and produces excellent data coverage (~99%) [20, 21].

This chapter provides a necessary step to derive accurate sea level anomaly (SLA) from AltiKa satellite altimetry. The framework developed in this chapter should enable the derivation of accurate sea levels over the Southeast Asia regions. The launched of the AltiKa satellite mission promises a significant refinement of coastal altimetry, with advanced instruments, an improved retracking algorithm, and geophysical corrections [7, 19, 20, 22, 23]. The validation and calibration of the satellite mission are compulsory to find the level of confidence on the data quality before it can be used in any applications. Global calibrations for AltiKa have been conducted by Centre National d’Etudes Spatiales (CNES), Indian Space Research Organization (ISRO), and many other researchers (e.g., [5, 19, 20, 24, 25]). However, limited research focuses on the regional validation over the Southeast Asia (e.g., [24, 26–29]). The regional validation is important because the ocean characteristics of the region are significantly different than the other oceans, such as the Pacific and Atlantic Ocean. It is characterized by marginal and semi-closed oceans that contain many small islands and a broad range of topographic features, thus producing complicated waveform patterns when they enter the altimeter footprints. Therefore, this study is conducted to quantify the quality of sea levels derived from the AltiKa over the Southeast Asia region.

This chapter presents the quality assessment, and the validation of AltiKa sea levels against tide gauges over the Southeast Asia coastal region. The quality assessment identifies how close the data can get to the coastline and how much data can be recovered through three retracking algorithms (i.e., MLE-4, Ice-1, and Ice-2) [30–32] Southeast. It is noted that the three retracking algorithms are the standard retrackers available from the Sensor Geophysical Data Records (SGDR). The assessments are conducted by computing: (1) the percentage of data availability over the Southeast coastal region; (2) the minimum distance of the AltiKa retracked sea level data to the coastline; and (3) the root mean square (RMS) error and temporal correlation of the retracked sea levels with tide gauges.

Section 2 presents the data description and processing procedures involved in the quality assessment and validation; Section 3 reports on the data qualitative assessment, which includes both the percentage of data availability and the minimum distance of sea level to the coastline; Section 4 reports on the validation of retracked sea levels against the tide gauge; and Section 5 concludes the chapter.

2. Data description and processing procedures

The experimental region encompasses the Southeast Asia, which comprises of the Andaman Sea, the Strait of Malacca, the Gulf of Thailand, the South China Sea, and the Sulu Sea (**Figure 2**). It covers an area of about 20°N–5°S and 95°E–126°E.

The data utilized in this study are acquired from several agencies. The altimeter data are available at the Archiving, Validation and Interpretation of Satellite Oceanographic Data (AVISO) ftp site (<ftp://avisoftp.cnes.fr>). SGDR product, which comprises of 40 Hz of data from cycles 1 to 19 (April 2013–December 2014), are utilized. Hourly tide gauge measurements are supplied by the Department of Survey and Mapping Malaysia (DSMM) and the University of Hawaii Sea Level Centre (UHSLC); <https://uhslc.soest.hawaii.edu>). There are six tide gauge stations used in this study, which are Geting, Langkawi, Bintulu, Lubang, Ko Taphao Noi, and Vung Tau (**Figure 2**). The hourly tide gauge data are acquired from March 2013 to December 2014.

For altimeter data, two processing steps are involved in the derivation of sea level: (1) by applying the range correction and (2) by correcting the impact of atmosphere and ocean geophysical. The range corrections are obtained from MLE-4, Ice-1, and Ice-2 retracking algorithms. The MLE-4 and Ice-2 algorithms are based on the theoretical model of scattering surface of Brown [10], and Ice-1 is the empirical method of the OCOG [15]. The geophysical amendments correct the SLAs by isolating the ocean dynamic height contributors of ocean tides, atmospheric refraction, and atmospheric pressure loading such as sea state bias (SSB) and inverse barometer.

The SLA from AltiKa is derived from Eq. (1) [33];

$$SLA = H - (R_{obs} - R_{retracked} - \Delta R_{wet} - \Delta R_{dry} - \Delta R_{iono} - \Delta R_{ssb} - mssh) - h_{ot} - h_{solid} - h_{pole} - h_{load} - h_{iny} - h_{hf} \quad (1)$$

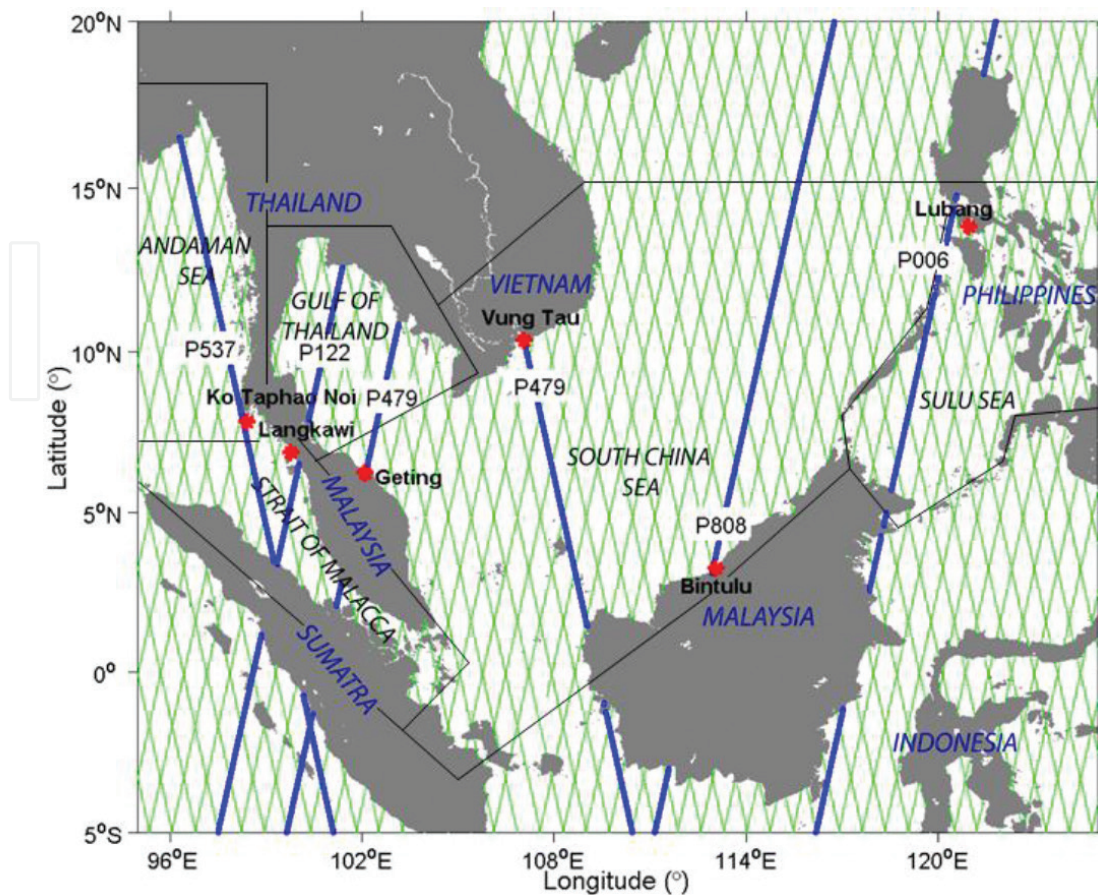


Figure 2. The region of the study area. Red marks indicate the tide gauge stations and green lines indicate the AltiKa ground passes. The blue lines are the AltiKa ground passes used for validation with tide gauge.

where H is satellite altitude, R_{obs} is the observed range, $R_{retracked}$ is the range corrections from the retracking algorithm (i.e., MLE-4, Ice-1 and Ice-2), R_{dry} and R_{wet} are dry and wet tropospheric corrections, R_{iono} is ionospheric correction, R_{ssb} is sea state bias correction, $mssh$ is mean sea surface height, h_{ot} is ocean tides, h_{solid} is solid earth tides, h_{pole} is pole tides, h_{load} is tidal loading, h_{iny} is inverse barometer height correction, and h_{hf} is high frequency fluctuations. The correction of R_{dry} and R_{wet} are based on the European Centre for Medium-Range Weather Forecasts, R_{iono} is from the Global Ionospheric Map, R_{ssb} is from the Hybrid sea state bias [34], and h_{ot} is from the FES2012 model. Due to limited number of data samples (~1.5 years) used in this study, the global FES2012 tidal model is used rather than a coastal tidal model such as the pointwise tide model (e.g., [35]). The use of pointwise tide modeling for resolving tidal signals requires at least 3 years of datasets to ensure that the individual constituents are separated due to the Rayleigh criterion [36]). It is noted that the use of the global tidal model to resolve coastal tidal signals may produce inaccurate results because tidal signals in the coastal regions are more complex than in the deep ocean.

The tide gauge data is processed to extract a non-tidal sea level time series, so that the physical contents are comparable to the satellite altimetry. The sea level measured by the tide gauge is different from the sea level measured by the satellite altimeter. The tide gauge measures the

changes in sea level over time relative to a datum, which is mean sea surface height (MSSH). Meanwhile, the altimeter measures the sea level above the reference ellipsoid.

The tide gauge is designed to estimate tides. In order to find the non-tidal sea level, high-frequency tidal effects on the tide gauge data need to be removed. Tidal signals from the tide gauge are removed using a harmonic analysis method [37, 38]. Harmonic analysis is a mathematical process which separates the observed tide into basic harmonic constituents. This method can determine the amplitude and phase of tidal constituents from a long-time series observation. It models the tidal signals as the sum of a finite set of sinusoids at specific frequencies related to astronomical parameters. If the amplitude and phase of each constituent is known, it can be removed from the sea level measurement [37].

3. Qualitative assessment

This section investigates the quantity of retracked SLAs from the three retrackers (i.e., MLE-4, Ice-1, and Ice-2) that are available from the AVISO SGDR product. The quantity is computed in terms of the percentage of data availability over the region (Section 3.1) and the minimum distance to the coastline (Section 3.2). These assessments are conducted to evaluate the amount of data that can be recovered through those three retracking algorithms.

3.1. Data availability of SARAL/AltiKa-retracked SLA over the coastal region

Figures 3–8 show the percentage of data availability over the regions. In general, the AltiKa shows an outstanding data recovery with $\geq 80\%$ of data availability for all retrackers (see **Figures 1–3**). The spatial plot around the Strait of Malacca shows that the data availability is considerably high ($\geq 70\%$) for most all passes of all retrackers, considering the complexity of the region with its narrow strait. However, several passes on the Andaman Sea show data availability of $\leq 70\%$. The percentage of data also degrades significantly over the eastern part of the Southeast Asia, around the Sulu Sea, near the Philippines coastal water. The data availability is $\leq 50\%$ for several passes.

The close-up of the most complex area around Singapore, near the Riau Archipelago, and the Sulu Sea near the Philippines, are shown in **Figures 6–8**. The percentage of data around the Riau Archipelago is considerably high ($\geq 70\%$) even though it is located in shallow water and surrounded by small islands. On the other hand, data over the Philippines coastal water degrades significantly with the percentage of data availability $\leq 50\%$ for several passes.

Figure 9 indicates the mean percentage of retracked SLA data availability within 30 km of the coastline for the five tested regions. Of all regions, the South China Sea has the highest ($\geq 88\%$) percentage, with the MLE-4, Ice-1, and Ice-2 retrackers providing 88, 90, and 89% of data, respectively. The South China Sea has less complex coastal topography when compared to the other regions. Hence, the contamination of land within the altimeter footprint may not be severe in this region, making the retracking of sea level work efficiently and producing outstanding data coverage.

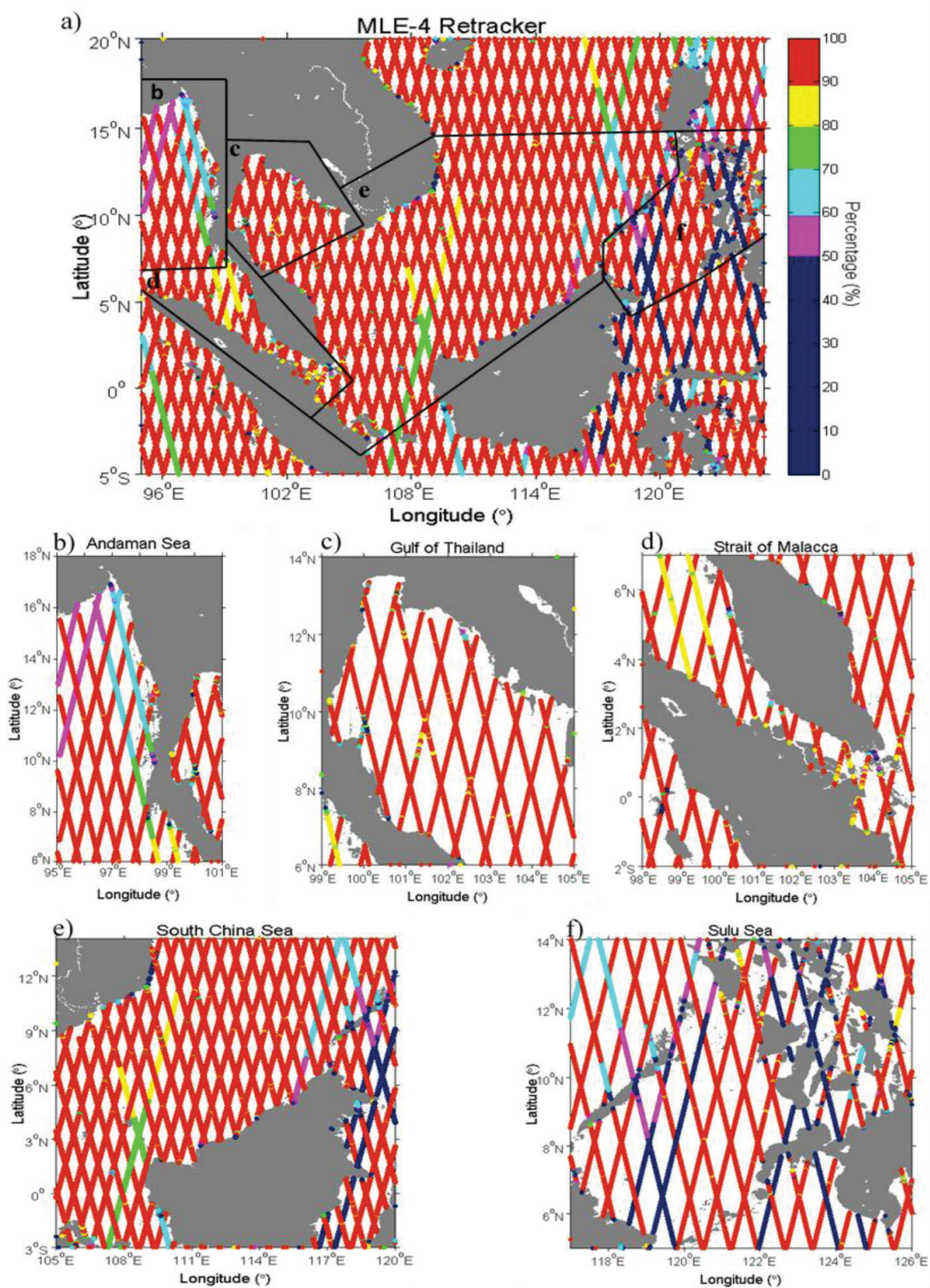


Figure 3. (a) The data availability (in unit %) for MLE-4 retracked SLAs over the Southeast Asia. Close up for (b) the Andaman Sea, (c) the Gulf of Thailand, (d) the Strait of Malacca, (e) the South China Sea, and (f) the Sulu Sea.

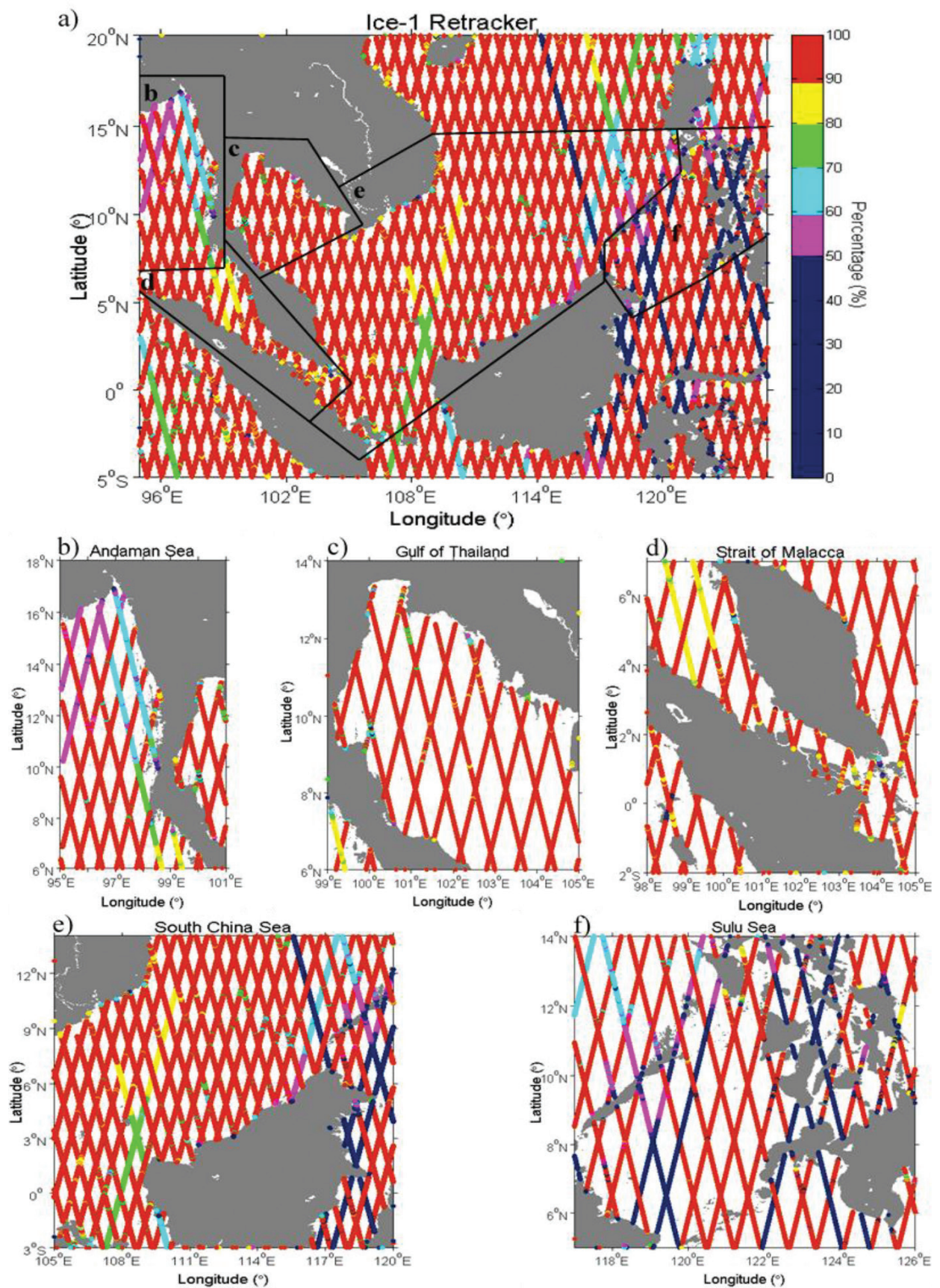


Figure 4. (a) The data availability (in unit %) for Ice-1 retracked SLAs over the Southeast Asia. Close up for (b) the Andaman Sea, (c) the Gulf of Thailand, (d) the Strait of Malacca, (e) the South China Sea, and (f) the Sulu Sea.

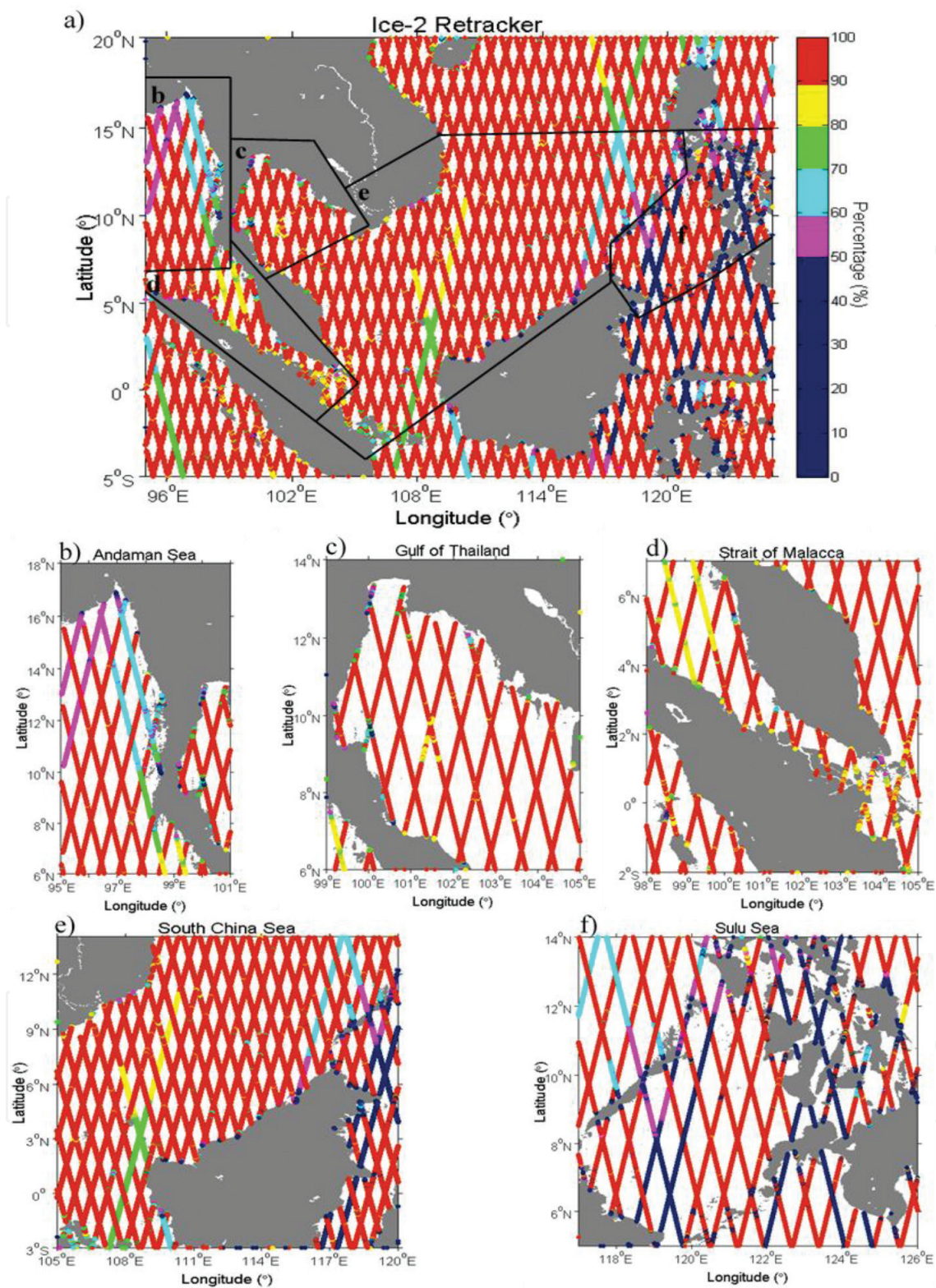


Figure 5. (a) The data availability (in unit %) for Ice-2 retracked SLAs over the Southeast Asia. Close up for (b) the Andaman Sea, (c) the Gulf of Thailand, (d) the Strait of Malacca, (e) the South China Sea, and (f) the Sulu Sea.

In contrast, the Sulu Sea has the lowest ($\leq 68\%$) percentage of data coverage, with the MLE-4, Ice-1 and Ice-2 retracker providing 64, 68, and 65% of data, respectively. The Sulu Sea is surrounded by many small islands, narrow straits, and shallow water with rough bottom topography. It is

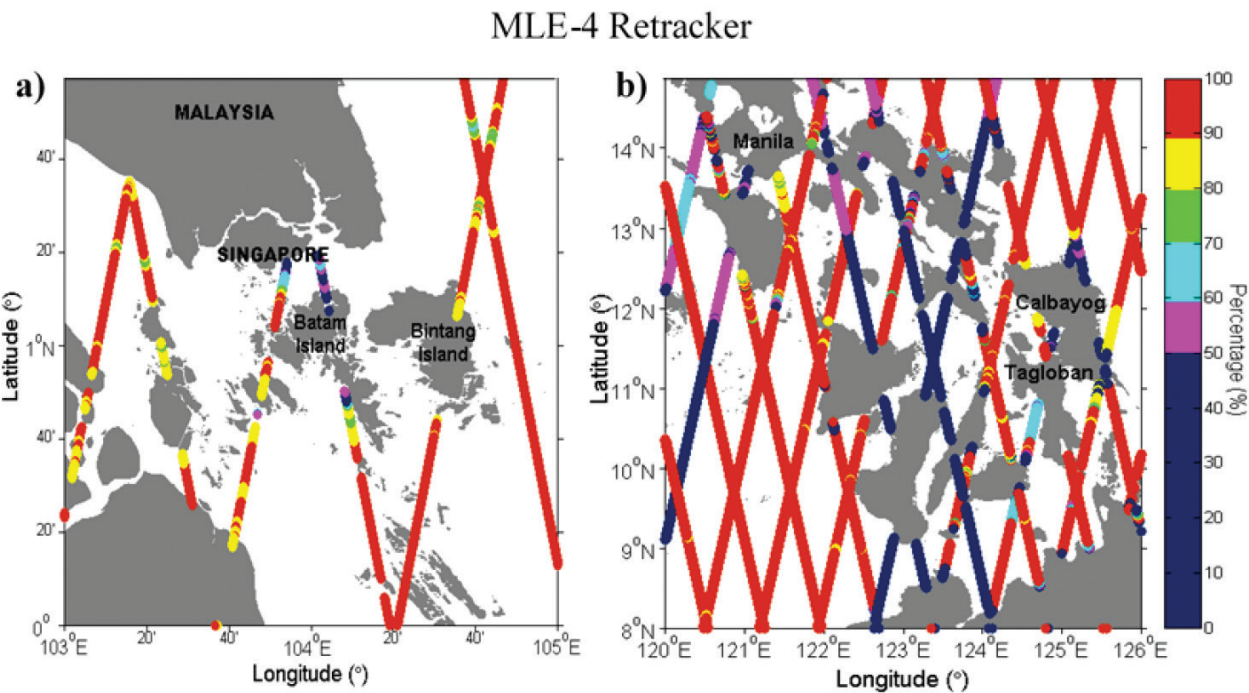


Figure 6. The data availability (in unit %) for MLE-4 retracked SLAs. Close up for area (a) near the Riau Archipelago and (b) over the Philippines coastal water.

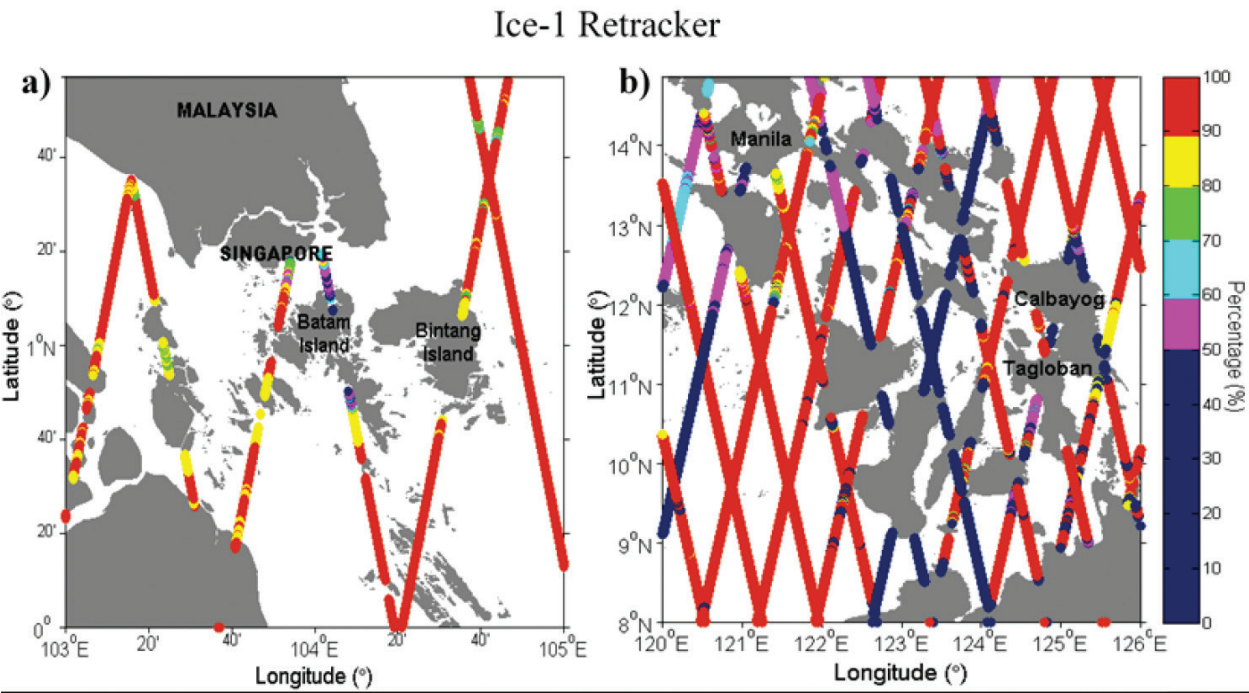


Figure 7. The data availability (in unit %) for Ice-1 retracked SLAs. Close up for area (a) near the Riau Archipelago and (b) over the Philippines coastal water.

one of the most complex archipelagos in the world [39]. This area also suffers from rapid changes in sea-state and quasi periodic-variation of surface roughness [40]. The altimetric waveforms could be severely corrupted due to the high complexity of the coastal topography, thus producing invalid estimations of geophysical information [8], particularly SLAs.

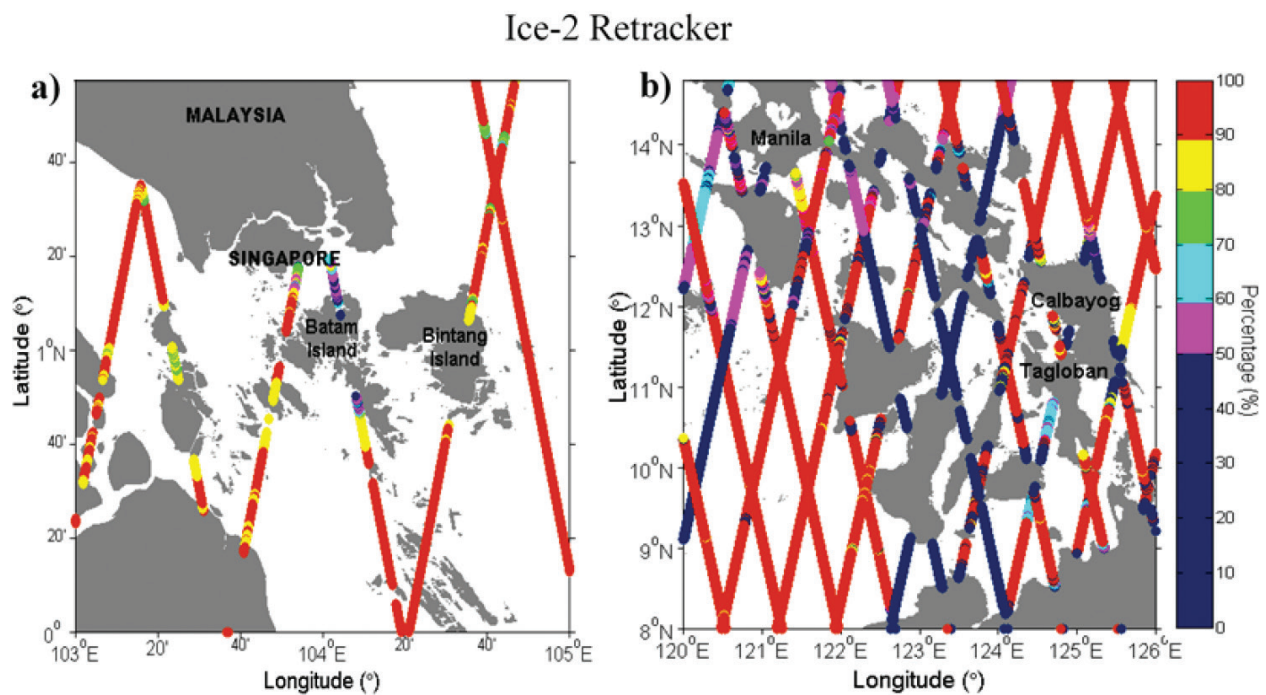


Figure 8. The data availability (in unit %) for Ice-2 retracked SLAs. Close up for area (a) near the Riau Archipelago and (b) over the Philippines coastal water.

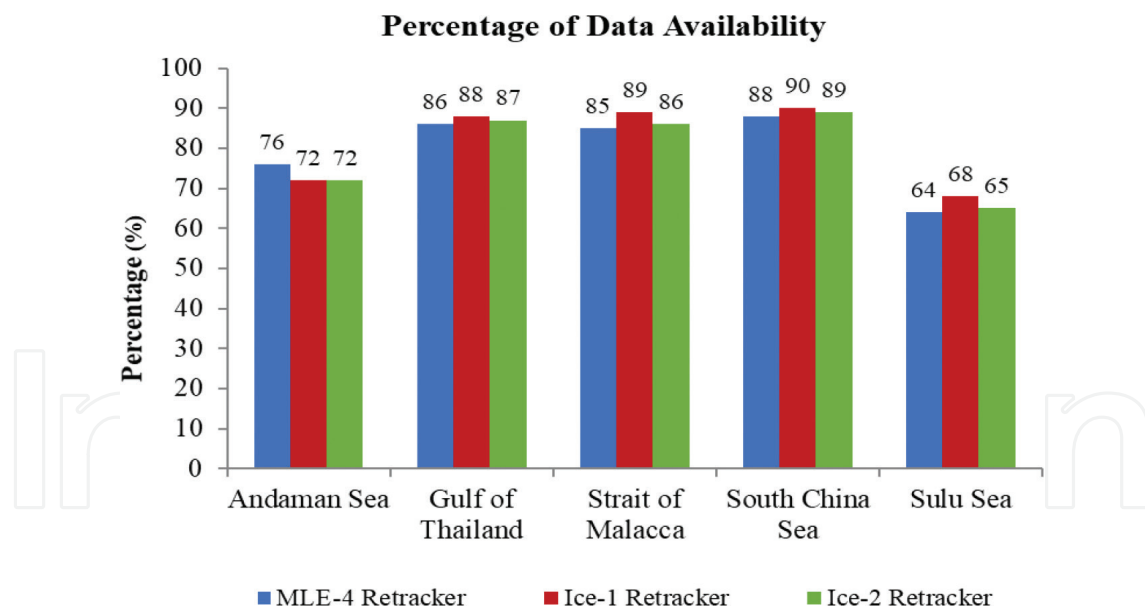


Figure 9. Mean percentage of AltiKa data availability over five experimental regions computed within 30 km of the coastline. It is computed from 18 passes for the Andaman Sea and the Strait of Malacca, 16 passes for the Gulf of Thailand, 30 passes for the South China Sea, and 17 passes for the Sulu Sea.

For the Andaman Sea, the Gulf of Thailand, and the Straits of Malacca, the AltiKa shows satisfactory results in data coverage with >72% data availability. Based on the result in **Figure 9**, 4 out of 5 regions have good data availability with more than 70% data coverage, thanks to the smaller AltiKa footprint size that has contributed to segregating the type of surface in transition zones (from water to land and from land to water) over coastal regions.

It is comprehended that the Ice-1 retracker always outperforms the MLE-4 and Ice-2 retrackers, except for the Andaman Sea where the performance of the Ice-1 and Ice-2 retrackers are similar. In contrast, the MLE-4 always underperforms compared to the other retrackers, except in the Andaman Sea where the percentage is slightly superior than those of other two retrackers.

3.2. The minimum distance of the SARAL/AltiKa retracked SLAs to the coastline

The quality of the AltiKa retracked SLAs over the coastal region is further investigated by computing the minimum distance of the available data to the coastline. **Figure 10** shows an example of the minimum distance of retracked AltiKa data computed from several passes over the Southeast Asia region. In general, the AltiKa SLAs data becomes available within 2 km from the coastline.

Figure 11 shows the mean minimum distance of the retracked AltiKa data computed over the five experimental regions. The total number of satellite passes included in the calculation is similar to the number of passes utilized in the computation of data availability. As shown in **Figure 11**, the AltiKa data over the South China Sea region have the lowest mean minimum distance compared to the other regions. The data are available within a distance of ≤ 3.2 km from the coastline. The Sulu Sea shows the opposite result, with the highest mean minimum distance ≥ 4 km from the coastline.

The finer spatial resolution with ~ 174 m along-track sampling in the Ka-band AltiKa (compared to the Jason-2 with ~ 300 m along-track sampling) enables high-density coastal observations, thus bringing the AltiKa measurements closer to the coastline. Based on previous research [21], this has confirmed that the AltiKa provides a significant improvement in accuracy and data availability up to ~ 3 km from the coastline. This is overwhelmingly better than the Jason-2 and Envisat which generally provide data beyond ~ 7 – 10 km from the coastline [18, 41, 42].

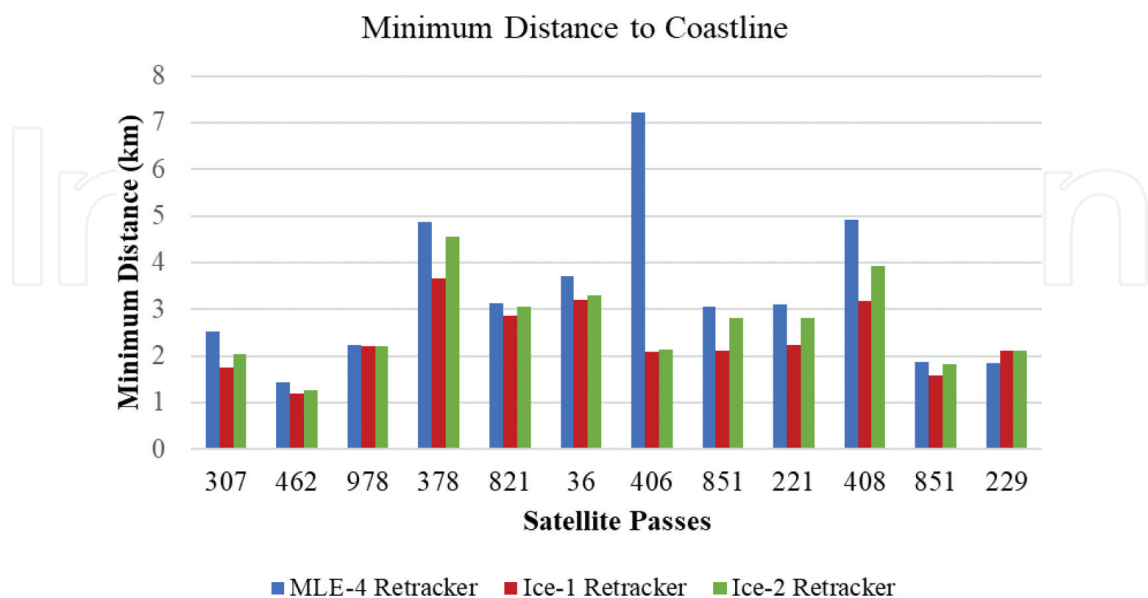


Figure 10. Mean of minimum distance of AltiKa MLE-4, Ice-1, and Ice-2 retracked SLAs to the coastline for several passes over the Southeast Asia coastal regions, computed from 19 cycles.

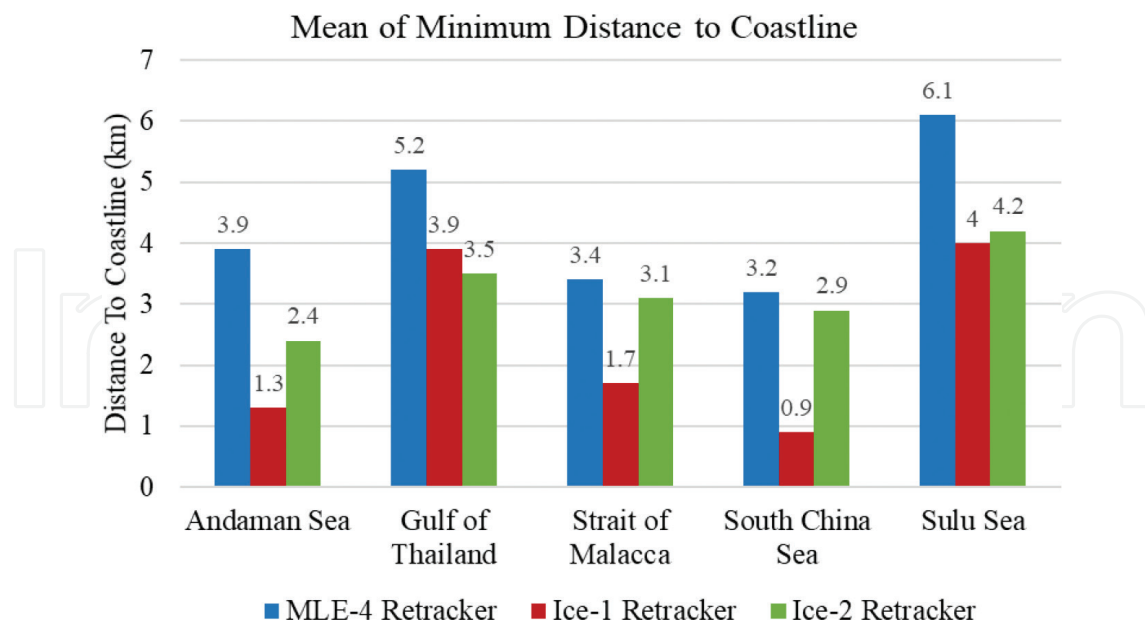


Figure 11. Mean of minimum distance of AltiKa for MLE-4, Ice-1 and Ice-2 retracked SLAs to the coastline over five experimental regions, computed from 19 cycles.

The overall inspection shows that the Ice-1 retracker performs better than other retracker within a minimum distance of ≤ 4 km from the coastline, except for in the Gulf of Thailand. Over this region, the Ice-2 retracker is better than the other retracker. The Ice-1 retracker is based on the OCOG, which is well-adapted to the rapidly changing surface like the continental sea shelf [8]. The MLE-4 retracker underperforms when compared to the other retracker, with a mean minimum distance of ≥ 3.2 km from the coastline. The MLE-4 retracker is the standard ocean retracker, which relies on the waveform's physical shape to fit the waveform to the theoretical Brown-shape [8, 12]. The Ice-2 retracker underperforms when compared to Ice-1 for most of the regions. However, the Ice-2 is better than the MLE-4 retracker. This is because the Ice-2 retracker is an adaptation of Brown's model, with slight modifications, and was purposely developed for continental ice regions, making it more adaptable for coastal waveforms.

4. Validation against tide gauge

To validate the AltiKa retracked SLA, the temporal correlation and RMS error between the SLAs from the retracking algorithms and tide gauges are calculated. In this study, the mean value of temporal correlation and RMS errors are computed for distances ≤ 5 km from the coastline. **Figure 12** shows the result for retracked SLAs from the MLE-4 Ice-1 and Ice-2 corresponding to the six tide gauge stations.

For the validation near Bintulu tide gauge, the MLE-4 retracker has better performance than those of Ice-1 and Ice2 retracker with a correlation of 0.53 and RMS error of 8 cm. The performance of Ice-1 and Ice-2 retracker is significantly low with correlation ≤ 4 and RMS error ≥ 13 cm. Near Geting station, the performance of three retracker are nearly similar, with

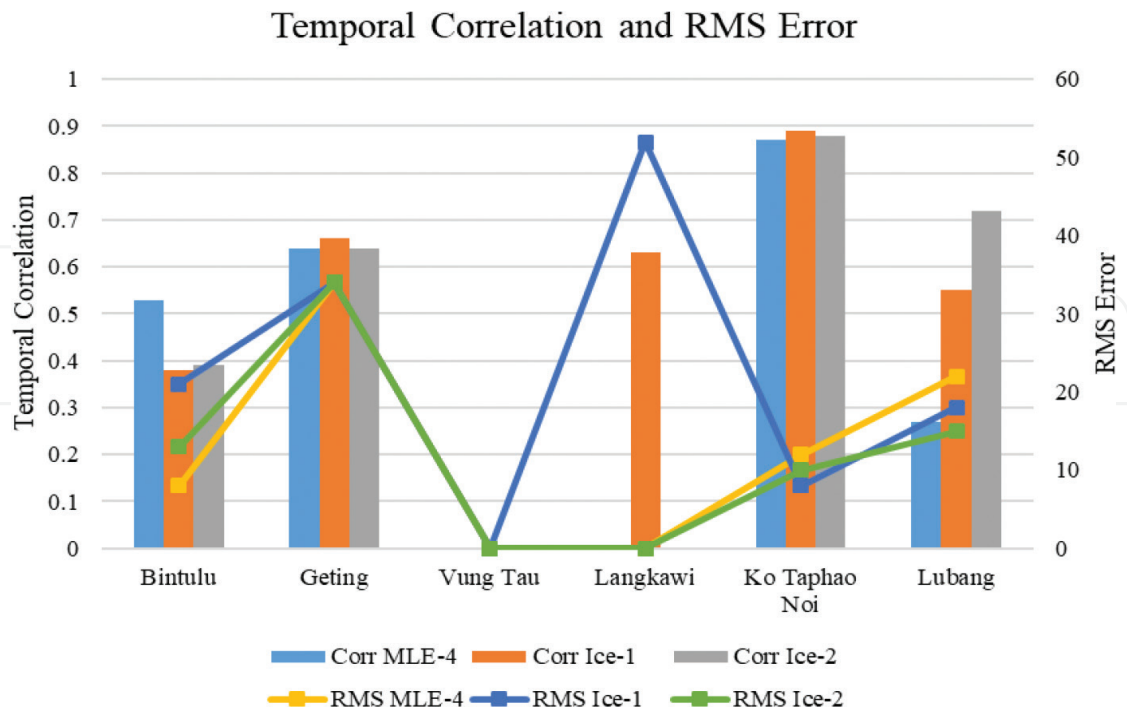


Figure 12. The temporal correlation and RMS error for MLE-4, Ice-1, and Ice-2 for distance within 5 km from coastline.

temporal correlation of 0.64 for MLE-4 and Ice-2 retrackerers and 0.66 for Ice-1 retracker, and RMS error of 34 cm for all retrackerers. Similar situation is shown near the Ko Taphao Noi tide gauge. The performance of three retracker are nearly similar with temporal correlation between 0.87 and 0.89 and RMS error between 8 and 12 cm. Near Vung Tau tide gauge, there is no data available for distance within 5 km from coastline. This is because, within this distance, satellite track crosses over a bay, thus producing complicated waveforms. The data over this area are unable to be retrieved from the three retracking algorithms. Near Langkawi tide gauge, the Ice-1 is the only retracker that can recover data. The temporal correlation and RMS error are 0.63 and 52 cm, respectively. Near Lubang tide gauge, Ice-2 is the optimum retracker based on the highest temporal correlation of 0.72 and RMS error 15 cm. The MLE-4 retracker seems to be the most inferior for this region, with a temporal correlation of 0.27 and an RMS error of 22 cm.

5. Summary

The AltiKa shows an excellent retracked SLA data coverage over the coastal water, with $\geq 85\%$ data availability for most locations of the experimental regions (three out of five regions). AltiKa measurements also can get as close as ~ 1 km from the coastline. This is extremely better than the performance of previous missions (i.e., Jason-2 and Envisat), which can generally provide measurements beyond $\sim 7\text{--}10$ km from the coastline.

For overall results, it shows that the Ice-1 is the optimum retracker over the Southeast Asia coastal region, with the percentage of data availability up to 90% and the minimum distance

as close as 0.9 km from the coastline. Nevertheless, the amount of data that can be recovered through the retracking algorithm depends on the coastal topography and sea states, in which different coastal characteristics have different impacts on the altimetric signals. Thus, this makes the performance of each retracker differ between different locations.

Acknowledgements

The research is supported by Research University Grant Tier 1 (vot 17H59). We would like to acknowledge the Ministry of Higher Education Malaysia for providing research funding. This acknowledgement also goes to the Achieving, Validating, and Interpretation of Satellite Oceanography (AVISO) data team for providing SARAL/AltiKa data, the Department of Survey and Mapping Malaysia (DSSM) and the University of Hawaii Sea Level Centre (UHSLC) for providing tide gauge data. Special thanks to Dr. Angela Maharaj from University of New South Wales, Australia for her constructive comment about this book chapter.

Author details

Noor Nabilah Abdullah¹ and Nurul Hazrina Idris^{1,2*}

*Address all correspondence to: nurulhazrina@utm.my

1 Faculty of Geoinformation and Real Estate, Universiti Teknologi Malaysia, Johor Bahru, Malaysia

2 Geoscience and Digital Earth Center, Research Institute for Sustainability and Environment, Universiti Teknologi Malaysia, Johor Bahru, Malaysia

References

- [1] Cipollini P, Snaith H. A short course on altimetry. In: 3rd ESA Advanced Training on Ocean Remote Sensing; 23-27 September. Cork, Ireland; European Space Agency; 2013
- [2] Anzenhofer M, Shum CK, Rentsch M, O.S. University. Coastal Altimetry and Application. Vol. 1. Columbus, Ohio: Department of Civil and Environmental Engineering and Geodetic Science; 1999
- [3] Challenor PG, Read JF, Pollard RT, Tokmakin RT. Measuring surface current in drake passage from altimetry and hydrography. *Journal of Physical Oceanography*. 1996;**26**: 2784-2758
- [4] Fu LL, Cazenave A, Fu LL, Cazenave A. Satellite Altimetry and Earth Sciences: A Handbook of Techniques and Applications. San Diego, California: Academic Press; 2001

- [5] Gómez-Enri J, Cipollini P, Gommenginger C, Martin-Puig C, Vignudelli S, Woodworth P, Benveniste J, Villares P. COASTALT: Improving radar altimetry products in the oceanic coastal area. *Remote Sensing of the Ocean, Sea Ice, and Large Water Regions*. 2008;**7**:1050J:1-10. DOI: 10.1117/12.802456
- [6] Bouffard J, Pascual A, Ruiz S, Faugère Y, Tintoré J. Coastal and mesoscale dynamics characterization using altimetry and gliders: A case study in the Balearic Sea. *Journal of Geophysical Research: Oceans*. 2010;**115**:1-17
- [7] Cipollini, P. The Coastal Zone: A Mission Target for Satellite Altimetry In *Coastal Altimetry Workshop*; 7-8 October; Boulder, Colorado; 2013. 72
- [8] Gommenginger C, Thibaut P, Fenodlio-Marc L, Quartly G, Deng X, Gomez-Enri J, Challenor P, Gao Y. Retracking altimeter waveforms near the coasts. A review of retracking methods and some applications to coastal waveforms. In Vignudelli S et al. *Coastal Altimetry*. London, New York: Springer; 2011. pp. 61-101. DOI: 10.1007/978-3-642-12796-0_4
- [9] Vignudelli S, Kostianoy AG, Cipollini P, Benveniste J. *Coastal Altimetry*. Berlin: Springer; 2011. DOI: 10.1007/978-3-642-12796-0.A
- [10] Brown GS. The average impulse response of a rough surface and its applications. *IEEE Journal of Oceanic Engineering*. 1977:67-74
- [11] Dinardo S, Benveniste J. Application of a modified brown model to quasi specular echoes. In *Coastal Altimetry Workshop*; 17-18 September; Frascati, Italy. 2009
- [12] Thibaut P, Poisson JC, Bronner E, Picot N. Relative performance of the MLE3 and MLE4 retracking algorithms on Jason-2 altimeter waveforms. *Marine Geodesy*. 2010;**33**:317-335. DOI: 10.1080/01490419.2010.491033
- [13] Brown S. A novel near-land radiometer wet path-delay retrieval algorithm: Application to the Jason-2/OSTM Advanced microwave radiometer. *IEEE Transactions on Geoscience and Remote Sensing*. 2010;**38**:1986-1992. DOI: 10.1109/TGRS.2009.2037220
- [14] Idris NH, Deng X, Md Din AH, Idris NH. CAWRES: A waveform retracking fuzzy expert system for optimizing coastal sea levels from Jason-1 and Jason-2 satellite altimetry data. *Remote Sensing*. 2017;**9**:603
- [15] Wingham DJ, Rapley CG, Griffiths H. New techniques in satellite tracking systems. In: *IGARSS. In 86 Symposium Digest*; September; Zurich, Switzerland. 1986. pp. 185-190
- [16] Villadsen H, Deng X, Andersen OB, Stenseng L, Nielsen K, Knudsen P. Improved inland water levels from SAR altimetry using novel empirical and physical retrackers. *Journal of Hydrology*. 2016;**537**:234-247
- [17] Deng X, Featherstone WE, Hwang C, Berry PAM. Estimation of constamination of ERS-2 and POSEIDON satellite radar altimetry close to the coasts of Australia. *Marine Geodesy*. 2002;**25**:249-271. DOI: 10.1080/01490410214990
- [18] Idris NH, Deng X. The retracking technique on multi-peak and quasi-specular waveforms for Jason-1 and Jason-2 missions near the coast. *Marine Geodesy*. 2012;**35**:217-237. DOI: 10.1080/01490419.2012.718679

- [19] Verron J, Sengenès P, Lambin J, Noubel J, Steunou N, Guillot A, Picot N, Coutin-Faye S, Sharma R, Gairola RM, Murthy DVAR, Richman JG, Griffin D, Pascual A, Remy F, Gupta PK. The SARAL/AltiKa altimetry satellite mission. *Marine Geodesy*. 2015;**38**:2-21. DOI: 10.1080/01490419.2014.1000471
- [20] Prandi P, Philipps S, Pignot V, Picot N. SARAL/AltiKa global statistical assessment and cross-calibration with Jason-2. *Marine Geodesy*. 2015;**38**:297-312. DOI: 10.1080/01490419.2014.995840
- [21] Abdullah NN, Idris NH, Maharaj AM. The retracked sea levels from SARAL/AltiKa satellite altimetry: The case study around the Strait of Malacca and the South China Sea. *International Journal of Geoinformatics*. 2016;**12**:33-39
- [22] Ratheesh S, Sharma R, Prasad KVSR, Basu S. Impact of SARAL/AltiKa-derived sea level anomaly in a data assimilative ocean prediction system for the Indian Ocean. *Marine Geodesy*. 2015;**38**:354-364. DOI: 10.1080/01490419.2014.988833
- [23] Schwatke C, Dettmering D, Börgens E, Bosch W. Potential of SARAL/AltiKa for inland water applications. *Marine Geodesy*. 2015;**38**:626-643. DOI: 10.1080/01490419.2015.1008710
- [24] Abdalla S. SARAL/AltiKa wind and wave products: Monitoring, validation and assimilation. *Marine Geodesy*. 2015;**38**:365-380. DOI: 10.1080/01490419.2014.1001049
- [25] Tournadre J, Poisson J, Steunou N, Picard B. Validation of AltiKa matching pursuit rain flag. *Marine Geodesy*. 2015;**38**:107-123
- [26] Abdullah NN, Idris NH, Idris NH. Performance of SARAL/Altika satellite altimetry mission over the Straits of Malacca and the South China Sea. In: *IEEE Workshop on Geoscience and Remote Sensing*; 16-17 November 2015. Kuala Lumpur, Malaysia; IEEE Geoscience and Remote Sensing Society Malaysia; 2015. pp. 86-89
- [27] Idris NH, Maharaj A, Abdullah NN, Deng X, Andersen OB. A comparison of Saral/Altika coastal altimetry and in-situ observation across australasia and maritime continent. In: *SARAL/AltiKa Workshop*; 27-31 October 2014. Lake Constant, Germany: ESA Publication; 2014
- [28] Idris NH, Maharaj A, Deng X, Abdullah NN, Idris NH, Wan Kadir WH. A comparison of Saral/Altika coastal altimetry and in-situ observation across australasia and maritime continent. In: *Australia Coastal Ocean Modelling and Observations*; 7-8 October 2014. Canberra, Australia: IMOS Australia; 2014
- [29] Mohammed SB, Idris NH, Abdullah NN. Along-track high resolution sea levels from SARAL/Altika satellite altimetry data over the maritime continent In: *IEEE Workshop on Geoscience and Remote Sensing*; 16-17 November. Kuala Lumpur, Malaysia: IEEE Geoscience and Remote Sensing Society Malaysia; 2015. pp. 90-93
- [30] Amarouche L, Thibaut P, Zanife OZ, Dumont JP, Vincent P, Steunou N. Improving the Jason-1 ground retracking to better account for attitude effects. *Marine Geodesy*. 2004;**27**:171-197. DOI: 10.1080/01490410490465210

- [31] Lee H, Shum CK, Emery W, Calmant S, Deng X, Kuo C-Y, Roesler C, Yi Y. Validation of Jason-2 altimeter data by waveform retracking over California coastal ocean. *Marine Geodesy*. 2010;**33**:304-316. DOI: 10.1080/01490419.2010.488982
- [32] Legresy B, Papa F, Remy F, Vinay G, Van Den Bosch M, Zanife O-Z. ENVISAT radar altimeter measurements over continental surfaces and ice caps using the ICE-2 retracking algorithm. *Remote Sensing of Environment*. 2005;**95**:150-163
- [33] Andersen OB, Scharroo R. Range and geophysical corrections in coastal regions: And implications for mean surface determination. In: Vignudelli S et al., editors. *Coastal Altimetry*. London, New York: Springer; 2011. pp. 103-146. DOI: 10.1007/978-3-642-12796-0
- [34] Wang D-P, Flagg CN, Donohue K, Rossby HT. Wavenumber spectrum in the gulf stream from shipboard ADCP observations and comparison with altimetry measurements. *Journal of Physical Oceanography*. 2010;**40**:840-844. DOI: 10.1175/2009jpo4330.1
- [35] Idris NH, Deng X, Andersen OB. The importance of coastal altimetry retracking and detiding: A case study around the Great Barrier Reef, Australia. *International Journal of Remote Sensing*. 2014;**35**:1729-1740
- [36] Andersen OB. Global ocean tides from ERS 1 and TOPEX/POSEIDON altimetry. *Journal of Geophysical Research: Oceans*. 1995;**100**:25249-25259
- [37] Pawlowicz R, Beardsley B, Lentz S. Classical tidal harmonic analysis including error estimates in MATLAB using T_TIDE. *Computers & Geosciences*. 2002;**28**:929-937
- [38] Schureman P. *Manual of Harmonic Analysis and Prediction of Tides*. US Government Printing Office; 1958
- [39] Brown RM, Siler CD, Oliveros CH, Esselstyn JA, Diesmos AC, Hosner PA, Linkem CW, Barley AJ, Oaks JR, Sanguila MB. Evolutionary processes of diversification in a model Island Archipelago. *Annual Review of Ecology, Evolution, and Systematics*. 2013;**44**:411-435
- [40] Apel JR, Holbrook JR, Liu AK, Tsai JJ. The Sulu Sea internal soliton experiment. *Journal of Physical Oceanography*. 1985;**15**:1625-1651
- [41] Babu K, Shukla A, Suchandra A, Arun Kumar S, Bonnefond P, Testut L, Mehra P, Laurain O. Absolute calibration of SARAL/AltiKa in Kavaratti during its initial calibration-validation phase. *Marine Geodesy*. 2015;**38**:156-170
- [42] Deng X, Featherstone WE. A coastal retracking system for satellite radar altimeter waveforms: Application to ERS-2 around Australia. *Journal of Geophysical Research*. 2006;**111**:12-28. DOI: 10.1029/2005jc003039